A Phase I, Open-Label, Dose-Escalation Study of the OX40 Agonist Ivuxolimab in Patients with Locally Advanced or Metastatic Cancers

Adi Diab[1], Omid Hamid[2], John A. Thompson[3], Willeke Ros[4], Ferry A.L.M. Eskens[5], Toshihiko Doi[6], Siwen Hu-Lieskovan[7], Samuel J. Klempner[8], Bishu Ganguly[9], Catherine Fleener[9], Xiao Wang[9], Tenshang Joh[9], Ken Liao[9], Shahram Salek-Ardakani[9], Carrie Turich Taylor[9], Jeffrey Chou[9], and Anthony B. El-Khoueiry[10]

ABSTRACT

Purpose: Stimulation of effector T cells is an appealing immunotherapeutic approach in oncology. OX40 (CD134) is a costimulatory receptor expressed on activated $CD4^+$ and $CD8^+$ T cells. Induction of OX40 following antigen recognition results in enhanced T-cell activation, proliferation, and survival, and OX40 targeting shows therapeutic efficacy in preclinical studies. We report the monotherapy dose-escalation portion of a multicenter, phase I trial (NCT02315066) of ivuxolimab (PF-04518600), a fully human immunoglobulin G2 agonistic monoclonal antibody specific for human OX40.

Patients and Methods: Adult patients ($N = 52$) with selected locally advanced or metastatic cancers received ivuxolimab 0.01 to 10 mg/kg. Primary endpoints were safety and tolerability. Secondary/exploratory endpoints included preliminary assessment of antitumor activity and biomarker analyses.

Results: The most common all-causality adverse events were fatigue (46.2%), nausea (28.8%), and decreased appetite (25.0%). Of 31 treatment-related adverse events, 30 (96.8%) were grade ≤2. No dose-limiting toxicities occurred. Ivuxolimab exposure increased in a dose-proportionate manner from 0.3 to 10 mg/kg. Full peripheral blood target engagement occurred at ≥0.3 mg/kg. Three (5.8%) patients achieved a partial response, and disease control was achieved in 56% of patients. Increased $CD4^+$ central memory T-cell proliferation and activation, and clonal expansion of $CD4^+$ and $CD8^+$ T cells in peripheral blood were observed at 0.1 to 3.0 mg/kg. Increased immune cell infiltrate and OX40 expression were evident in on-treatment tumor biopsies.

Conclusions: Ivuxolimab was generally well tolerated with on-target immune activation at clinically relevant doses, showed preliminary antitumor activity, and may serve as a partner for combination studies.

Introduction

Blocking immune checkpoints with monoclonal antibodies (mAb) is an established approach that has improved survival across multiple cancer types. However, not all patients respond, and late relapses (acquired resistance) are observed during longer-term follow-up of responders (1). The mechanisms of immune escape are complex and actively studied in patients and preclinical models in order to develop effective salvage and upfront treatment strategies (2).

Approved approaches have focused on blocking the inhibitory effects of checkpoint receptors. For example, checkpoint molecules such as programmed cell death 1 (PD-1) and CTL-associated protein 4 (CTLA-4) negatively regulate T-cell activation. However, the direct stimulation of effector T cells is an attractive and complementary approach. OX40 (CD134, TNFRSF4) is a potent costimulatory protein in the tumor necrosis factor receptor superfamily (3). OX40 can be induced on the surface of activated $CD4^+$ and $CD8^+$ T cells, but is not found on resting naïve T cells or most resting memory T cells (4–9). OX40 engagement is involved in T-cell survival (10, 11), clonal expansion of naïve T cells (12), generation of effective T-cell responses (13–18), and suppression of the activity of regulatory T cells (19–21). It is also reported that neoadjuvant OX40 administration increases T-cell infiltration to the tumor microenvironment (22, 23). Furthermore, OX40 regulates cytokine production from T cells and cytokine receptor signaling and promotes T-cell memory (16, 24). Inhibition of tumor growth using agonistic OX40 mAbs and OX40 ligands has been found in preclinical models of melanoma, sarcoma, glioma, colon, breast, prostate, and renal cancers (25–29).

Ivuxolimab (PF-04518600) is a fully human immunoglobulin (Ig) G2 agonistic mAb specific for human OX40. Unlike IgG1-based approaches, ivuxolimab does not induce antibody-dependent cellular cytotoxicity and does not deplete OX40-expressing cells. Upon binding to OX40 on activated tumor-infiltrating T cells, ivuxolimab may

[1]Department of Melanoma Medical Oncology, The University of Texas MD Anderson Cancer Center, Houston, Texas. [2]Immuno-Oncology and Cutaneous Malignancies, The Angeles Clinic and Research Institute, a Cedars-Sinai Affiliate, Los Angeles, California. [3]Division of Medical Oncology, University of Washington School of Medicine/Seattle Cancer Care Alliance, Seattle, Washington. [4]Department of Pharmacology, Netherlands Cancer Institute, Amsterdam, the Netherlands. [5]Department of Medical Oncology, Erasmus MC Cancer Institute, Rotterdam, the Netherlands. [6]Department of Gastrointestinal Oncology, National Cancer Center Hospital East, Kashiwa, Chiba, Japan. [7]Division of Hematology-Oncology, Department of Medicine, University of California, Los Angeles (UCLA), Los Angeles, California. [8]Department of Medicine, Massachusetts General Hospital Cancer Center, Boston, Massachusetts. [9]Pfizer, New York, New York. [10]Norris Comprehensive Cancer Center, University of Southern California, Los Angeles, California.

Corresponding Author: Adi Diab, UT MD Anderson Cancer Center, 1400 Holcombe Boulevard, Faculty Center Room Fc11.3004, Houston, TX 77030. Phone: 713-745-7336; Fax: 713–745–1046; E-mail: ADiab@mdanderson.org

Clin Cancer Res 2022;28:71–83

doi: 10.1158/1078-0432.CCR-21-0845

Translational Relevance

Preclinical studies in animal models have demonstrated that agonistic engagement of OX40 (CD134, TNFRSF4), a potent costimulatory protein in the tumor necrosis factor receptor superfamily, positively regulates $CD4^+$ and $CD8^+$ T-cell activity and can suppress the activity of regulatory T cells, with effective antitumor responses. To assess whether OX40 engagement may provide a novel strategy to improve tumor control in patients, we evaluated the OX40 agonist monoclonal antibody ivuxolimab (PF-04518600) in a phase I, open-label, dose-escalation study. Ivuxolimab was generally well tolerated at the doses evaluated (up to 10 mg/kg every 2 weeks) with no dose-limiting toxicities and mostly grade 1 to 2 treatment-related adverse events. Preliminary evidence of antitumor activity was observed, with partial responses in 2 patients with melanoma and 1 patient with hepatocellular carcinoma, and disease control rate of 56%.

enhance tumor immunity. Here we describe the dose-escalation portion of the first-in-human phase I study of ivuxolimab in patients with locally advanced or metastatic cancers. Analysis from preplanned biomarker studies is presented in parallel to support the immunomodulatory effects of ivuxolimab.

Patients and Methods

Study design and endpoints

This was an open-label, multicenter, phase I study (ClinicalTrials.gov identifier: NCT02315066). Adult patients ($N = 52$) with head and neck squamous cell carcinoma (HNSCC), hepatocellular carcinoma (HCC), malignant melanoma (MEL), or renal cell carcinoma (RCC) received ivuxolimab intravenously once every 2 weeks. Six dose levels were examined: 0.01, 0.1, 0.3, 1.5, 3, and 10 mg/kg.

Primary endpoints determined safety and tolerability to define dose-limiting toxicities (DLT) and maximum tolerated dose (MTD). A modified toxicity probability interval method (30), targeting a DLT rate of 25% and an acceptable DLT interval (20%–30%) was used for dose escalation. A DLT observation period of 28 days was required for dose escalation; safety and tolerability assessments for the first 98 days to assess any late immune-related adverse events (AE) were taken into account for MTD. Secondary endpoints included pharmacokinetics (PK), antidrug antibodies (ADA), neutralizing antibodies (NAb), antitumor clinical activity, and target engagement of ivuxolimab. Exploratory endpoints included pharmacodynamic activity in blood and the tumor microenvironment.

The study was approved by the institutional review board or independent ethics committee of the participating institutions and conducted in accordance with legal and regulatory requirements, as well as the general principles set forth in the International Ethical Guidelines for Biomedical Research Involving Human Subjects (Council for International Organizations of Medical Sciences 2002), Guidelines for Good Clinical Practice (International Council for Harmonisation of Technical Requirements for Pharmaceuticals for Human Use 1996), and the Declaration of Helsinki (World Medical Association 1996 and 2008). In addition, the study was conducted in accordance with the protocol and applicable local regulatory requirements and laws. Written informed consent was obtained from all patients. The manuscript was developed from an open database with a data cutoff date of May 30, 2018.

Patients

Patients were ages ≥18 years with a histologically or cytologically proven diagnosis of HNSCC, HCC, MEL, or RCC, and at least one measurable lesion as defined by Response Evaluation Criteria in Solid Tumors (RECIST) v1.1; an Eastern Cooperative Oncology Group performance status 0–1; and adequate renal, bone marrow, liver, and cardiac function. Patients were not eligible if they had symptomatic brain metastases requiring steroids, a history of or active autoimmune disorders, were receiving systemic immunosuppression, or had received previous high-dose chemotherapy requiring stem-cell rescue or previous treatment with an OX40 agonist. Prior therapy with anti–PD-1, anti–PD-L1, and anti–CTLA-4 antibodies was allowed.

Treatment

Patients received ivuxolimab every 2 weeks in escalating intravenous doses of 0.01, 0.1, 0.3, 1.5, 3, and 10 mg/kg. The starting dose was based on the minimum anticipated biological effect level. Each cohort included an initial safety cohort of 2 to 4 patients per dose group, with a staggered start, and tumor biopsy backfill cohorts. After 28 days (two cycles), escalation to the next dose level occurred.

Safety

AEs were graded by NCI Common Terminology Criteria for Adverse Events v.4.03. Late immune-related DLTs (immune-related AEs that meet the same grading criteria as DLT criteria, and occurring to day 98 of the assessment period) were also taken into account.

Pharmacokinetics and immunogenicity

Blood samples for PK evaluation were collected pre- and post-dose and analyzed for ivuxolimab using a validated electrochemiluminescent (ECL) assay. PK parameters were calculated by noncompartmental methods using internally validated software (eNCA, v2.2.4). Samples below the lower limit of quantification (LLOQ) were set to zero for analysis. Serum samples for immunogenicity evaluation were assayed for ADA using a validated ECL assay. Samples tested positive for ADA were analyzed for NAbs using a validated cell-based assay.

Pharmacodynamics

CD4 and CD8 central ($CD45RA\text{-}CCR7^+$) and effector ($CD45RA\text{-}CCR7^-$) memory T-cell subsets were measured by flow cytometry. Proliferation was assessed using ki67, and T-cell activation by measuring coexpression of HLA-DR and CD38. The levels of proliferation and activation markers on memory T-cell subsets were compared with those on naïve T cells, which express significantly lower levels of OX40. Patient samples with baseline frequencies <2% for activation or proliferation markers (LLOQ for the assay) were excluded.

Blood samples taken pre- and posttreatment were analyzed within 48 hours. Blood (200 μL) was stained with anti-CD3 Alexa Fluor 488 (BioLegend), anti-CD4 PE/Cy7 (BioLegend), CD45RA PerCP/Cy5.5 (BioLegend), and anti-CCR7 BV-510 (BioLegend; core-staining cocktail). For receptor occupancy, Alexa Fluor 647–labeled anti-OX40 clone 19B10 (Pfizer proprietary reagent; binds competitively with ivuxolimab) or Alexa Fluor 647–labeled anti-OX40 clone 16C4 (Pfizer proprietary reagent; binds noncompetitively with ivuxolimab) was added to the cocktail to measure free or total OX40. For T-cell activation analysis, 200 μL of blood was incubated with the core-staining cocktail containing anti–HLA-DR BV421 (BD Biosciences) and anti-CD38 PE (BioLegend). Blood samples were lysed and fixed and then resuspended in BD Stain Buffer (BD Biosciences). For T-cell proliferation analysis, 200 μL of heparinized blood was incubated with

the core-staining cocktail for 30 minutes; blood samples were lysed and fixed, washed, and permeabilized with BD Perm Buffer 2 (BD Biosciences), then incubated with anti-ki67 Alexa Fluor 647. Samples were washed and resuspended in BD Stain Buffer for analysis. Flow-cytometric profiles were analyzed by counting 100,000 $CD3^+$ events on a FACSCanto 10 analyzer with FACSDiva software (BD Biosciences). Data were graphed using Prism (GraphPad Software).

Peripheral blood TCRβ sequencing

$CD4^+$ and $CD8^+$ cells were sorted from peripheral blood samples from all cohorts at baseline; cycle 4, day 1; and cycle 7, day 1. DNA was extracted for sequencing of the TCRβ chain complementarity-determining region 3 (CDR3). Immunosequencing of the CDR3 regions of human TCRβ chains was performed using the immunoSEQ Assay (Adaptive Biotechnologies).

Tumor IHC

Paired biopsy samples were collected at baseline and after 6 weeks of ivuxolimab treatment across five dose cohorts ($n = 15$) of patients with HCC ($n = 8$), MEL ($n = 3$), HNSCC ($n = 3$), and RCC ($n = 1$). Formalin-fixed paraffin-embedded sections were analyzed by a research-use-only IHC assay and automated image analysis algorithm developed and validated at Flagship Biosciences. CD8, CD4, FoxP3, and OX40 protein expression in tumor biopsy samples was measured at baseline and cycle 4, day 1.

Subcutaneous tumor models in mice

Six- to 8-week-old female Balb/c mice (Jackson Laboratories) were housed in a pathogen-free facility at Rinat/Pfizer Inc. Experiments were conducted according to protocols in accordance with the Institutional Animal Care and Use Committee guidelines.

Mice were inoculated subcutaneously (both flanks) with 1×10^5 CT26 cells in 0.1 mL phosphate-buffered saline. When tumor volume reached 70 to 100 mm^3, mice were randomized to the anti-OX40 group and the isotype control antibody group. Treatment began 24 hours following surgery. Tumor size was measured using digital calipers, and the volume expressed in cubic millimeters using the formula $V = 0.5 \times (L \times W^2)$, where L and W are the long and short diameters of the tumor, respectively. Body weights were recorded weekly. Percentage of tumor growth inhibition was defined as $[1 - (\text{Tumor volume}_{\text{Treated}}/\text{Tumor volume}_{\text{Isotype control}})] \times 100$. Percentage of weight loss was defined as $[1 - (\text{Body weight}_{\text{Treated}}/\text{Body weight}_{\text{Isotype control}})] \times 100$.

Tumor RNA sequence analysis

RNA sequencing (RNA-seq) of tumor samples was conducted at Personalis Inc. Sequencing alignment and gene-expression quantification was performed using OmicSoft ArraySuite software. DESeq2 (31) was used for paired differential analysis on eight paired biopsies from patients dosed with >1.5 mg/kg ivuxolimab. Genes were ranked from most upregulated to downregulated by test statistic calculated by DESeq2. Fast preranked gene set enrichment analyses FGSEA (32) were performed on the ranked genes using Hallmark gene sets for gene set enrichment analysis (33).

For RNA-seq analysis of the CT26 preclinical model, sequencing alignment and gene-expression quantification were performed using OmicSoft ArraySuite software (QIAGEN). Paired differential analyses were performed by DESeq2 on nine pairs of pretreatment and post-treatment tumor samples from responders and nine pairs of samples from isotype controls, separately. The difference between the changes in responders and the changes in isotype controls ranked the genes for gene set enrichment analysis by FGSEA.

Antitumor activity

Radiologic assessment of antitumor activity was conducted every 6 weeks until confirmed progressive disease (PD). Scans could be moved to every 12 weeks after 24 weeks until confirmed PD. The study assessed tumor response using RECIST v1.1.

Results

Patients and exposure

A total of 52 patients with HNSCC, HCC, MEL, or RCC received ivuxolimab intravenously once every 2 weeks in six dose-escalation groups: 0.01 mg/kg ($n = 2$), 0.1 mg/kg ($n = 10$), 0.3 mg/kg ($n = 11$), 1.5 mg/kg ($n = 12$), 3 mg/kg ($n = 13$), and 10 mg/kg ($n = 4$; **Table 1**). Most (82.7%) patients were male. The mean age was 60 years (range, 23–79). Nineteen (36.5%) patients had a primary diagnosis of HCC, 15 (28.8%) MEL, 9 (17.3%) RCC, and 9 (17.3%) HNSCC. Median duration of exposure to ivuxolimab was 71.5 days (range, 1–770). Twenty-one (40%) patients had received checkpoint inhibitor therapy (anti–PD-1, anti–PD-L1, or anti–CTLA-4), 25 (48%) prior chemotherapy, and 12 (23%) prior therapy with tyrosine kinase inhibitors.

Safety

No DLTs were observed across the dose range (0.01–10 mg/kg). The most common all-causality AEs (≥25%) were fatigue (46.2%), nausea (28.8%), and decreased appetite (25.0%; Supplementary Table S1). Thirty-one (59.6%) patients experienced treatment-related AEs. Thirty AEs (96.8%) were grade ≤2, with, the most frequent (≥5%) being fatigue (25.0%); influenza-like illness, pruritus, and vomiting (7.7% each); and decreased appetite, headache, and nausea (5.8% each). One (1.9%) patient experienced immune-related AEs of elevated gamma-glutamyl transferase and alkaline phosphatase, and hypothyroidism (all grade ≤2). One episode of asymptomatic grade 3 increase in gamma-glutamyl transferase was reported as a treatment-related AE in the ivuxolimab 1.5 mg/kg cohort. There was one episode of grade 2 congestive cardiac failure in the 0.1 mg/kg cohort. This was not a myositis episode, and data currently available from nonclinical safety pharmacology do not suggest treatment-related effects on cardiovascular endpoints. This patient had ongoing risk factors including type 2 diabetes mellitus, transient ischemic attack, hypertension, carotid stenosis, and hypercholesterolemia, and history of prior exposure to doxorubicin, which may have affected cardiac function (34). The majority of patients ($n = 31$; 59.6%) discontinued treatment due to disease progression or relapse. The next most common reasons for discontinuation were a global deterioration of health status ($n = 8$; 15.4%) and treatment-unrelated AEs ($n = 5$; 9.6%).

Pharmacokinetics and immunogenicity

PK assessments included all 52 patients at the 0.01, 0.1, 0.3, 1.5, 3, and 10 mg/kg dose levels once every 2 weeks. Full PK profiles were obtained for 0.1 mg/kg and above. At the 0.1 mg/kg dose, ivuxolimab PK exhibited a pattern consistent with target-mediated drug disposition compared with higher doses (Supplementary Fig. S1). Between doses of 0.3 and 10 mg/kg, exposure to ivuxolimab increased in an approximately dose-proportional manner (Supplementary Table S2). Following multiple infusions of ivuxolimab once every 2 weeks, the mean accumulation ratio ranged from 1.4 to 2.1 (Supplementary Table S2).

Immunogenicity assessments included all 52 patients treated with ivuxolimab with at least one ADA sample. Of 51 patients with baseline ADA samples, 4 (7.8%) tested positive for ADA; no patient tested

Table 1. Patient characteristics and summary of BOR and duration of responses by dose (RECIST).

	Ivuxolimab dose						
Cohort	**0.01 mg/kg *n* = 2**	**0.1 mg/kg *n* = 10**	**0.3 mg/kg *n* = 11**	**1.5 mg/kg *n* = 12**	**3 mg/kg *n* = 13**	**10 mg/kg *n* = 4**	**Total *N* = 52**
Age, mean (range), years	53 (48–57)	58 (40–79)	52 (23–67)	68 (54–78)	62 (45–75)	60 (41–74)	60 (23–79)
Sex, *n* (%)							
Male	1 (50.0)	8 (80.0)	8 (72.7)	11 (91.7)	11 (84.6)	4 (100)	43 (82.7)
Female	1 (50.0)	2 (20.0)	3 (27.3)	1 (8.3)	2 (15.4)	0	9 (17.3)
ECOG PS, *n* (%)							
0	1 (50.0)	6 (60.0)	7 (63.6)	4 (33.3)	6 (46.2)	2 (50.0)	26 (50.0)
1	1 (50.0)	4 (40.0)	4 (36.4)	8 (66.7)	7 (53.8)	2 (50.0)	26 (50.0)
Treatment duration, median (range), days	43.5 (29–58)	71.5 (27–183)	74.0 (29–770)	50.0 (27–281)	98 (1–225)	162 (1–555)	71.5 (1–770)
Primary diagnosis[a], *n* (%)							
HCC	1 (50)	6 (60)	3 (27)	6 (50)	3 (23)	0	19 (37)
MEL[b]	1 (50)	2 (20)	4 (36)	3 (25)	4 (31)	1 (25)	15 (29)
RCC	0	2 (20)	3 (27)	2 (17)	2 (15)	0	9 (17)
HNSCC	0	0	1 (9)	1 (8)	4 (31)	3 (75)	9 (17)
Number of prior systemic therapies, mean (range)	4.5 (2–7)	2.8 (1–11)	3.3 (1–10)	3.8 (1–8)	3.5 (1–8)	2.3 (1–3)	3.3 (1–11)
Number of prior immunotherapies, *n* (%)							
Anti–CTLA-4	1 (50)	2 (20)	2 (18)	3 (25)	3 (23)	1 (25)	12 (23)
Anti–PD-1	1 (50)	3 (30)	5 (45)	4 (33)	3 (23)	2 (50)	18 (35)
Anti–PD-L1	0	0	0	0	0	1 (25)	1 (2)
Other immunotherapy	0	1 (10)	0	1 (8)	0	0	2 (4)
BOR, *n* (%)							
CR	0	0	0	0	0	0	0
PR	0	1 (10.0)	1 (9.1)	0	0	1 (25.0)	3 (5.8)
SD	0	5 (50.0)	6 (54.5)	6 (50.0)	8 (61.5)	1 (25.0)	26 (50.0)
PD (%)	2 (100.0)	3 (30.0)	4 (36.4)	6 (50.0)	3 (23.1)	1 (25.0)	19 (36.5)
Indeterminate (%)	0	1 (10.0)	0	0	0	0	1 (1.9)
NE (%)	0	0	0	0	2 (15.4)	1 (25.0)	3 (5.8)
Mean DOR, weeks	—	10.3	93.1	—	—	35.9	46.4
Mean DOSD, weeks	—	11.1	13.0	18.0	13.9	30.0	14.7
Median time to first PD, weeks	5.8	11.8	7.6	6.2	12.4	36.1	11.6

Note: Time to first PD is defined as time from start of treatment until date of first PD or the last non-PD assessment date prior to cutoff date.
Abbreviations: BOR, best overall response; CR, complete response; DOR, duration of response; DOSD, duration of SD; ECOG PS, Eastern Cooperative Oncology Group performance status; HCC, hepatocellular carcinoma; HNSCC, head and neck squamous cell carcinoma; MEL, malignant melanoma; NE, not evaluable; PD, progressive disease; PR, partial response; RCC, renal cell carcinoma; SD, stable disease.
[a]Since metastatic diagnosis.
[b]0.01 mg/kg: $n = 1$ cutaneous; 0.1 mg/kg: $n = 1$ cutaneous, $n = 1$ other; 0.3 mg/kg: $n = 2$ cutaneous, $n = 1$ acral, $n = 1$ other; 1.5 mg/kg: $n = 2$ cutaneous, $n = 1$ acral; 3.0 mg/kg: $n = 2$ cutaneous, $n = 1$ uveal, $n = 1$ other; 10 mg/kg: $n = 1$ cutaneous.

positive for NAb at baseline. Of 50 patients with at least one post-dose ADA sample, 15 (30%) tested positive for treatment-induced ADA and none had treatment-boosted ADA; 8 (of 15) patients had transient ADA detected at no more than two sampling time points. The median time to onset of ADA was 14 days. Three (6%) patients tested positive for treatment-induced NAb.

The majority of ADA responses had no effect on PK, particularly at dose levels ≥0.3 mg/kg; however, the presence of NAb (only observed at the 0.1 mg/kg dose level) was associated with lower trough concentrations (C_{trough}; Supplementary Fig. S2A). Specifically, the C_{trough} levels were similar between ADA^+ and ADA^- samples, except that at the 0.1 mg/kg dose level, a few ADA^+ samples with high titer or with NAb^+ status also had lower C_{trough}. Furthermore, at the 0.1 mg/kg dose level, 2 patients with sustained high NAb titers (log_{10} of NAb titer >0.5) had lower C_{trough} compared with expected profiles (Supplementary Fig. S2B). One of the NAb^+ patients achieved a partial response (PR) while NAb was detected, but subsequently had disease progression owing to a new lesion. The immunogenicity response was not associated with anaphylaxis or other hypersensitivity reactions.

Pharmacodynamics

Using an anti-OX40 antibody that binds competitively with ivuxolimab, free OX40 levels were assessed by flow cytometry as a measure of peripheral target engagement. Free OX40 levels decreased with increasing dose, and ivuxolimab exhibited full target engagement at doses ≥0.3 mg/kg, measured on central memory CD4 T cells (CD4 TCM cells; **Fig. 1A**). Full receptor saturation for the dosing duration was observed in a patient with a PR in the 0.1 mg/kg cohort (**Fig. 1B**).

Total OX40 levels were monitored using an anti-OX40 antibody that binds noncompetitively with ivuxolimab. OX40 levels were generally unchanged in the periphery following dosing with ivuxolimab, measured on CD4 central and effector memory cells at cycle 1, day 1 (predose); cycle 2, day 1; and cycle 4, day 1 (time of tumor biopsy). See **Fig. 1C** for CD4 central memory cells.

The effects of ivuxolimab on activation and proliferation of peripheral blood T cells were assessed by monitoring changes in HLA-DR and CD38 coexpression, and intracellular ki67 expression on memory T cells (**Fig. 2**). These responses were compared with those observed on naïve T cells, where minimal to no measurable OX40 expression was detected (**Fig. 2E**). Increased proliferation was observed on $CD4^+$

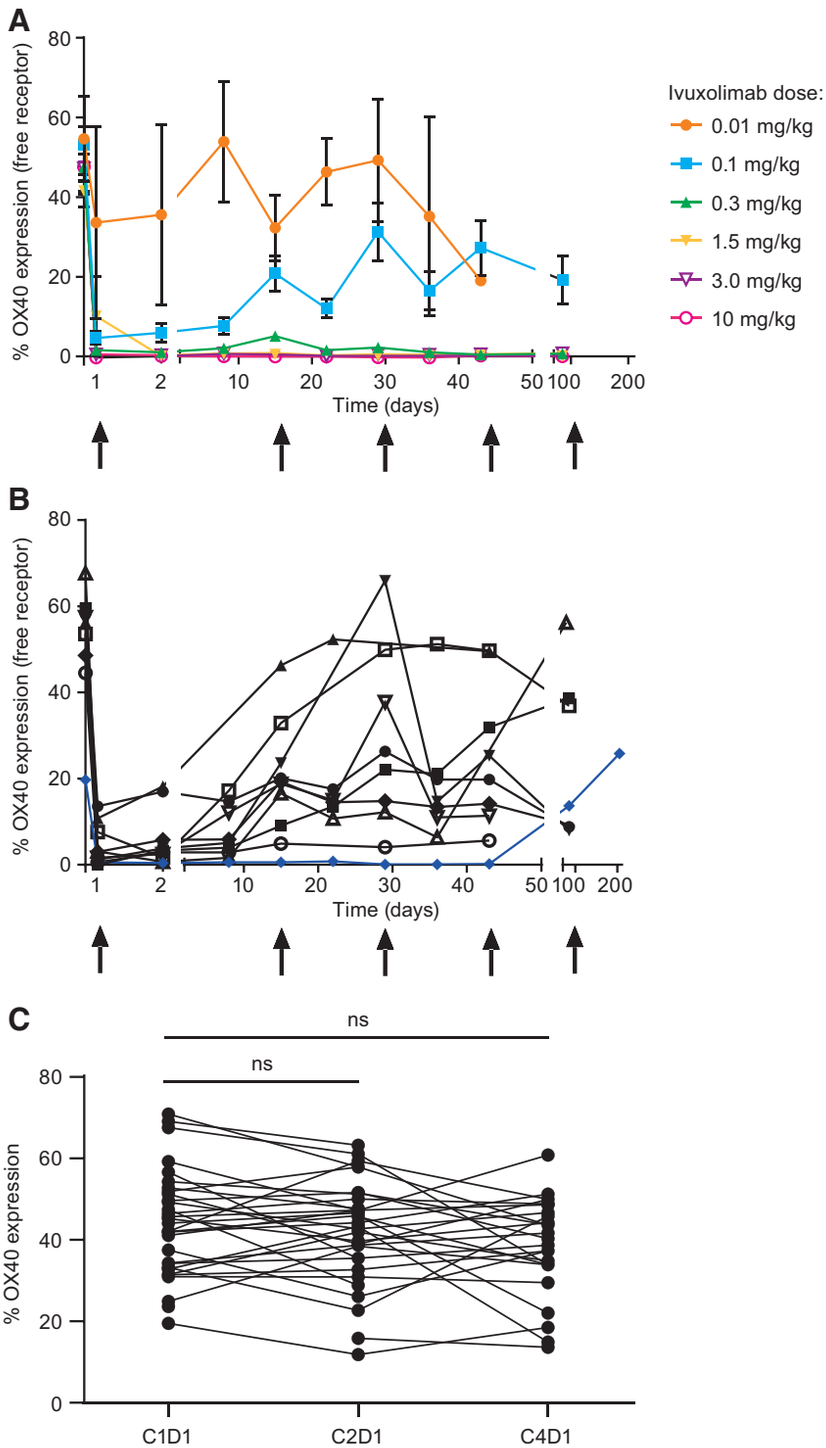

Figure 1.

A, Peripheral receptor occupancy measurement demonstrates dose-dependent changes in free OX40 receptor levels. Peripheral blood samples collected at baseline; weekly through cycle 4, day 1; and at cycle 7, day 1 were stained with a fluorescent-labeled competitive anti-OX40 antibody. These data represent the percent of CD4 central memory T cells expressing the OX40 receptor pre- and posttreatment at each dose level. **B,** Receptor saturation for the dosing duration. Full receptor occupancy (blue line) was observed in one patient in the 0.1 mg/kg cohort who had a PR. **C,** Total OX40 levels were generally unchanged in the periphery following dosing with ivuxolimab.

effector and central memory T cells, most frequently at the 0.1, 0.3, and 3 mg/kg doses at 2 weeks post-dose (cycle 2, day 1), with a trend for the most consistent responses at the 0.3 mg/kg dose level, in contrast to naïve T cells where no increase in proliferation was observed. Similar results were found when assessing T-cell activation, although maximal increases in activation appeared at later time points than for proliferation (cycle 4, day 1, 6 weeks post-dose). Fold change in the proliferation and activation markers ranged from 1.5- to 3-fold with no apparent dose response, with diminished peripheral responses at 10 mg/kg. Consistent with lower but measurable levels of OX40 on these subsets, $CD8^+$ memory T cells showed modest but variable increases in proliferation and activation markers, with similar kinetics to those observed for $CD4^+$ memory T cells (**Fig. 2A–E**). PD-1 levels in the periphery increased in some patients at doses where increased

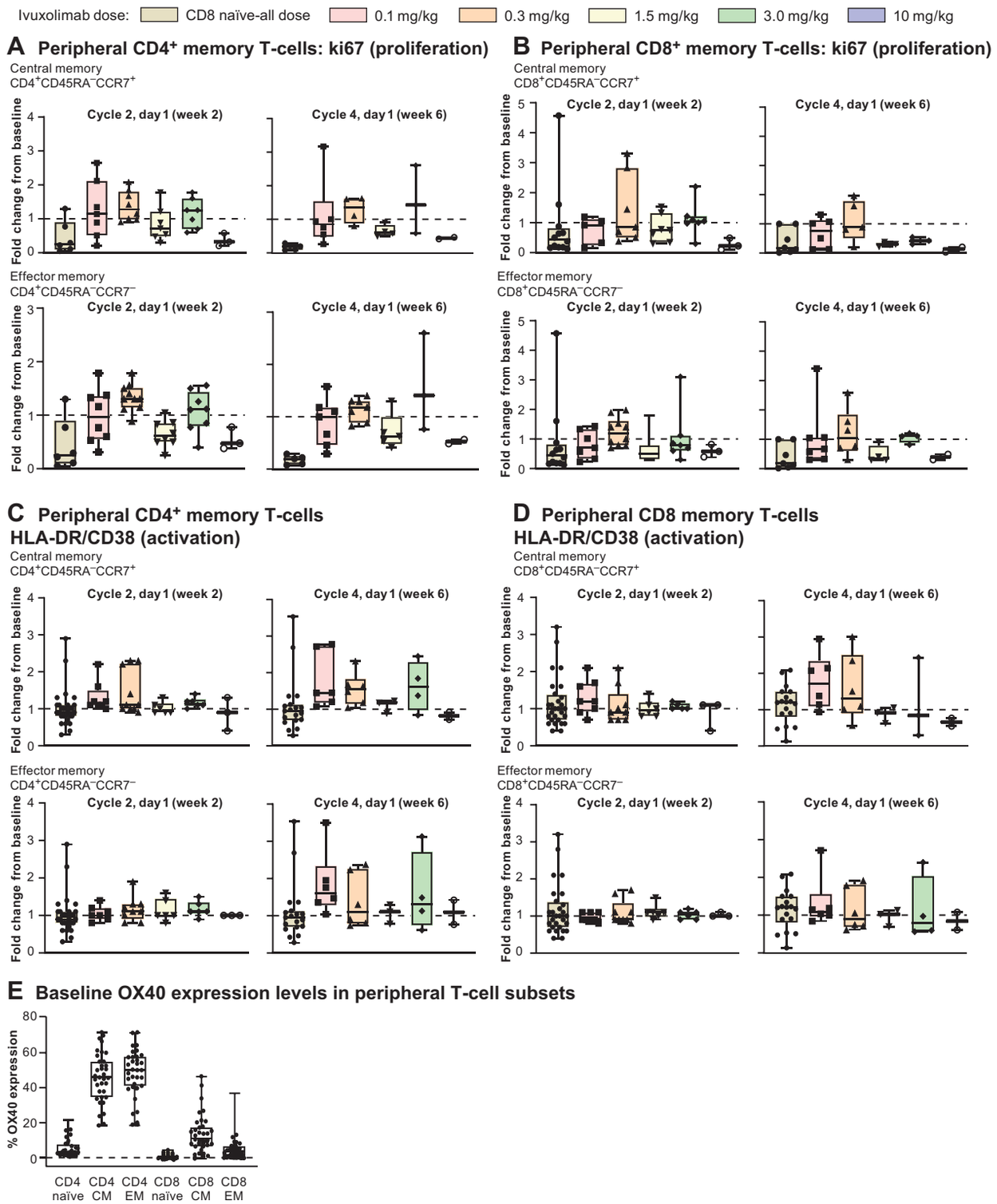

Figure 2.

A, Changes in proliferation of $CD4^+$ memory T cells assessed by ki67. **B,** Changes in proliferation of $CD8^+$ memory T cells assessed by ki67. **C,** Activation markers HLA-DR/CD38 on $CD4^+$ memory T cells. **D,** Activation markers on $CD8^+$ memory T cells. **E,** Baseline OX40 expression in peripheral T-cell subsets.

proliferation and activation were observed (data not shown). Regulatory T cells (Treg) and OX40 levels on Treg were also measured, but no significant changes in Treg frequencies or OX40 expression levels were observed (data not shown). There was no correlation between levels of peripheral T-cell activation or proliferation and clinical response.

Peripheral blood TCRβ sequencing

The objective of peripheral blood TCRβ sequencing was to build upon the observation of peripheral blood T-cell proliferation and activation by flow cytometry, to investigate the effect of ivuxolimab on TCR sequence diversity and clonal expansion. Because OX40 is known to be expressed transiently on antigen-experienced memory T cells, clonal expansion may be observed in a limited subset of T-cell clones.

TCRβ sequencing revealed clonal expansion of $CD4^+$ and $CD8^+$ T cells at dose levels 0.1 to 3.0 mg/kg from baseline to week 6 of ivuxolimab dosing. On average, $CD8^+$ T cells had a higher number of expanded clones than $CD4^+$ T cells (Supplementary Fig. S3). Patients in the 0.1–3.0 mg/kg dose groups with PR had among the lowest levels of normalized T-cell clonal expansion in the peripheral blood (Supplementary Fig. S4). This was especially apparent in the $CD8^+$ T-cell populations. However, some nonresponding patients also demonstrated low levels of normalized T-cell clonal expansion. The median numbers of expanded clones were similar for patients with stable disease (SD) or PD (Supplementary Fig. S4). TCRβ sequencing data are accessible at clients.adaptivebiotech.com/pub/diab-2021-ccr; DOI:10.21417/AD2021CCR.

Tumor IHC

A positive correlation between changes in tumor OX40 expression and time to progression (TTP) was observed in a limited sample set (**Fig. 3A**). TTP did not exhibit any correlation with baseline or fold-change expression of CD8, CD4, or FoxP3. Fold change from baseline in the expression of CD8, FoxP3, CD4, and OX40 in tumor tissue did not associate with dose or tumor type in the limited ($n = 12$) set of biopsies. Pathology review of IHC images indicated that, in addition to lymphocytes, endothelial cells stained positive for OX40 (**Fig. 3B**).

Tumor RNA sequence analysis

Combined RNA-seq data from eight paired tumor biopsies from patients dosed with ≥1.5 mg/kg ivuxolimab were submitted for FGSEA. Hallmark gene sets associated with immune activation and inflammation were among the most enriched (highest positive normalized enrichment score with the lowest adjusted *P* values; **Fig. 4A**). This pattern was not observed if samples from lower dose cohorts (0.1 and 0.3 mg/kg) were included. Paradoxically, tumor response assessment at the same time point (∼6 weeks) indicated clinical responses at these lower doses, suggesting persistent enrichment of immune-related transcripts may not be required for antitumor activity.

The significance of these gene-expression changes to the antitumor mechanism of action of ivuxolimab is further supported by the observation that the three most enriched gene sets in the >1.5 mg/kg dose cohort clinical samples were identical to those enriched in tumor samples collected from a CT26 syngeneic mouse tumor model. In this model, an ivuxolimab surrogate antibody exhibited robust antitumor activity (**Fig. 4B**). The gene sets in question, interferon-gamma (IFNγ) response, allograft rejection, and IFNα response, are associated with antitumor immune response. RNA sequence data are deposited to GEO, accession #GSE184752.

Antitumor activity

PR was observed in 3 patients (one HCC and two cutaneous MEL), whereas 26 patients had SD and 19 had PD as the best response; 3 were not evaluable for response and 1 was indeterminate. Disease control rate (DCR), which includes CR/PR/SD, occurred in 56% of patients (**Table 1**; Supplementary Table S3; **Fig. 5A**). Twenty-two (42%) patients had received prior immunotherapy, 21 of whom had received prior anti–PD-1, anti–PD-L1, or anti–CTLA-4 treatment. When comparing patients who had not received prior checkpoint inhibitors ($n = 31$) with those who had ($n = 21$), a similar DCR (58.1% vs. 52.4%) and median duration of SD (11.7 weeks, range, 5.4–37.4 weeks vs. 12.1 weeks, range, 6.0–30.0 weeks) were observed. Median TTP trended slightly better for patients without prior checkpoint inhibitors (11.6 weeks, range, 5.3–104.4 weeks) versus those who had taken prior checkpoint inhibitors (7.6 weeks, range, 5.4–79.1 weeks). One patient with cutaneous MEL (ivuxolimab 0.1 mg/kg) had a PR at cycle 10 (day 127) until cycle 14 (day 198). This was the only patient at 0.1 mg/kg with full OX40 receptor occupancy. This patient had received prior high-dose IFNα, high-dose interleukin-2, and ipilimumab combined with nivolumab before ivuxolimab. One patient with HCC (ivuxolimab 0.3 mg/kg) had received sorafenib for 2 months prior, achieving a best overall response (BOR) of SD while on sorafenib. This patient had a PR while receiving ivuxolimab lasting from cycle 6 (day 80) until cycle 51 (day 731), without drug-related toxicities.

One patient with cutaneous MEL in the 10 mg/kg cohort had previously received ipilimumab and pembrolizumab before enrollment and both were stopped due to toxicity (the BOR for these treatments was PD). This patient tolerated ivuxolimab well, and at cycle 6, the overall response was SD. After receiving 5,000 centigrays of focal stereotactic body radiotherapy (SBRT 1250 centigrays × 4 fractions) due to an oligoprogressing nontarget lung lesion, vitiligo developed bilaterally on the forearms, outside and far from the radiation field (**Fig. 5B**). In subsequent restaging scans, a mesenteric melanoma lesion distant from the radiation field decreased in size. The numerical decrease was –16% and –27% from baseline at cycles 10 and 12, respectively. This patient achieved a durable PR at cycle 14 (day 212) of ivuxolimab lasting until cycle 31 (day 462), with PD by cycle 36.

Discussion

The OX40 agonistic mAb ivuxolimab was generally well tolerated in this first-in-human dose-escalation study, throughout a dose range of 0.01 to 10 mg/kg, with no DLTs. Most treatment-related AEs were low grade and did not appear to be dose-dependent, and only one patient reported immune-related AEs. This is in contrast with the high probability of immune-mediated toxicity observed with checkpoint inhibitor therapy. Exposure was dose-proportional between 0.3 and 10 mg/kg. Ivuxolimab exhibited full peripheral blood target engagement in all patients at all doses ≥0.3 mg/kg, as indicated by the measurement of free OX40 on CD4 TCM cells. As seen for other OX40 agonists (23, 35, 36), there was evidence of activation and proliferation of memory T cells in response to ivuxolimab, particularly at 0.1 and 0.3 mg/kg. The fold change in activation and proliferation markers in peripheral blood ranged from 1.5- to 3-fold at these doses, similar to those observed for the OX40 mAb 9B12 study and with similar kinetics, where ki67 increases were reported in $CD4^+FoxP3_{neg}$ T cells from cryopreserved peripheral blood mononuclear cells (PBMC; ref. 35). There was also modest $CD4^+$ and $CD8^+$ T-cell clonal expansion in peripheral blood, with $CD8^+$ cells exhibiting higher median levels of expansion, although the antigen to which the clonally expanded T cells were responding to is not known. The

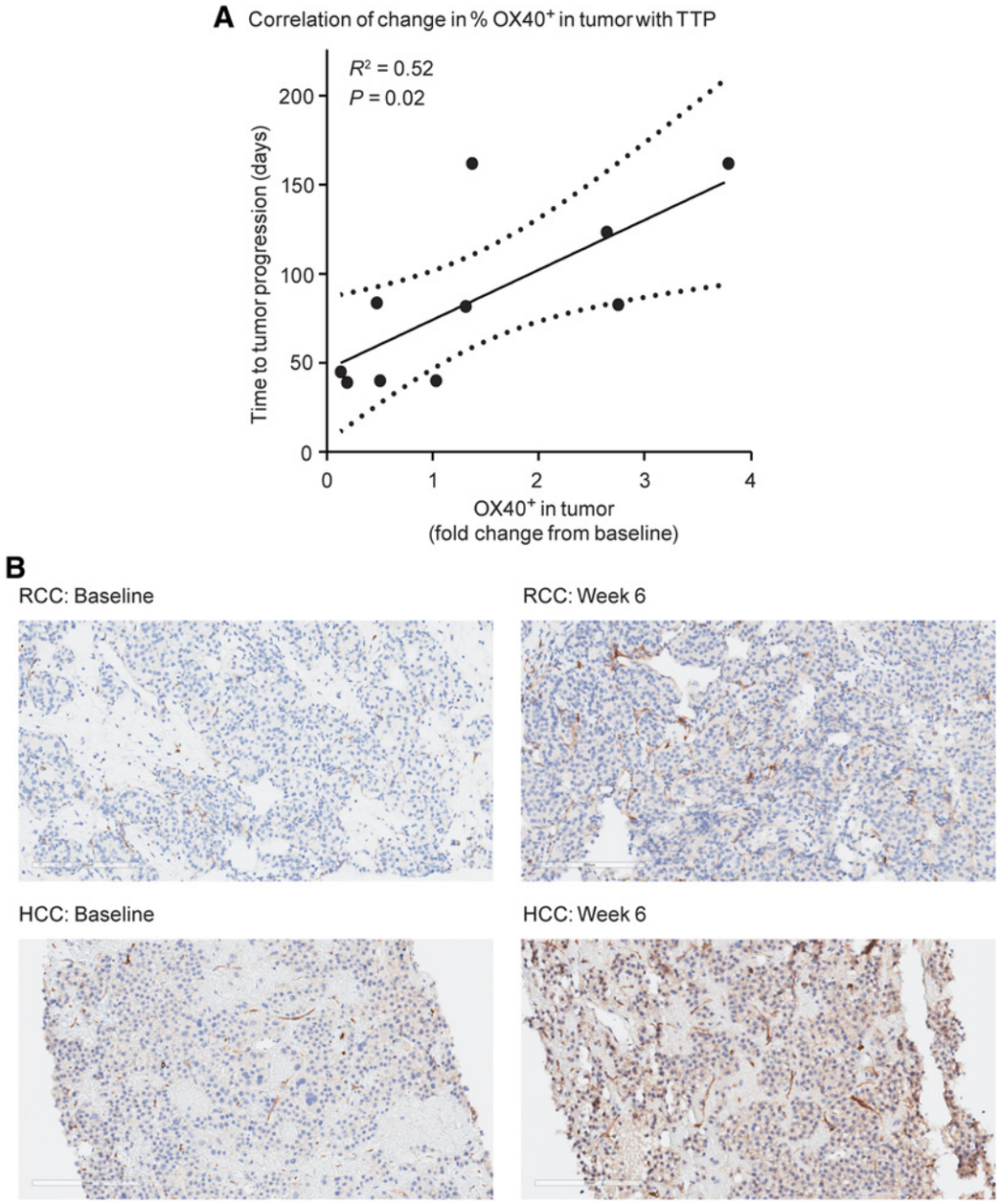

Figure 3.

A, A positive correlation between changes in tumor OX40 expression and TTP was observed in a limited sample set. TTP did not exhibit any correlation with baseline or fold-change expression of CD8, CD4, or FoxP3. **B,** Examples of OX40-positive staining at baseline and week 6 in a patient with RCC and a patient with HCC. 20× magnification. 4-μm sections were stained with anti-CD134 clone ACT-35 murine IgG1 antibody (BD catalog #555836).

responder at 0.1 mg/kg was the only patient at this dose with full receptor occupancy. These findings suggest higher receptor occupancy may be required for optimal activity with ivuxolimab than has been reported for BMS-986178, a fully human IgG1 OX40 receptor antibody, which appears to have an optimal receptor occupancy of 20% to 50% for maximal T-cell effector function, and decreased OX40 surface expression when receptor occupancy is >40% (37). However, similar to BMS-986178, T-cell activation appeared more prominent at lower doses (0.1 and 0.3 mg/kg) of ivuxolimab. The diminished peripheral responses at the 10 mg/kg dose could reflect a hook effect, whereby less efficient ivuxolimab binding at higher concentrations results in a diminished PD effect. The natural ligand, OX40L, binds to OX40 as a trimer. To optimize OX40 signaling, ivuxolimab would need to mimic this trimeric structure, which may be more difficult at high mAb concentrations. Also, two of three responses were observed at 0.1 and 0.3 mg/kg. The remaining response occurred at 10 mg/kg after the patient received palliative radiotherapy. No loss in total OX40 surface expression from peripheral T cells was observed with ivuxolimab,

A

Pathway	Gene ranks	NES	*P*	P_{adj}
ALLOGRAFT REJECTION		2.21	1.6e–05	6.5e–04
INTERFERON GAMMA RESPONSE		1.74	3.1e–05	6.5e–04
INFLAMMATORY RESPONSE		1.68	6.2e–05	6.5e–04
KRAS SIGNALING UP		1.68	6.2e–05	6.5e–04
MYC TARGETS V1		1.66	7.8e–05	6.7e–04
MYOGENESIS		1.63	1.1e–04	7.1e–04
HEME METABOLISM		1.63	1.6e–04	9.0e–04
OXIDATIVE PHOSPHORYLATION		1.62	1.9e–04	9.7e–04
XENOBIOTIC METABOLISM		1.59	3.1e–04	1.5e–03
MTORC1 SIGNALING		1.58	4.0e–04	1.8e–03
PI3K–AKT–MTOR SIGNALING		1.68	4.6e–04	1.8e–03
IL2–STAT5 SIGNALING		1.47	2.3e–03	7.5e–03
COMPLEMENT		1.42	5.7e–03	1.6e–02
REACTIVE OXYGEN SPECIES PATHWAY		1.58	8.7e–03	2.3e–02
KRAS SIGNALING DN		1.34	1.8e–02	4.0e–02

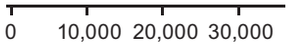

B

Pathway	Gene ranks	NES	*P*	P_{adj}
INTERFERON GAMMA RESPONSE		2.14	1.0e–05	1.7e–04
ALLOGRAFT REJECTION		1.82	1.0e–05	1.7e–04
INTERFERON ALPHA RESPONSE		2.13	1.1e–05	1.7e–04
MYOGENESIS		1.56	7.1e–05	7.4e–04
COMPLEMENT		1.52	9.1e–05	7.9e–04
INFLAMMATORY RESPONSE		1.49	4.4e–04	2.9e–03
XENOBIOTIC METABOLISM		1.44	1.3e–03	6.8e–03
IL2–STAT5 SIGNALING		1.43	1.7e–03	7.2e–03
KRAS SIGNALING DN		1.40	4.0e–03	1.5e–02
ESTROGEN RESPONSE LATE		1.32	1.6e–02	4.3e–02
IL6–JAK–STAT3 SIGNALING		1.41	1.7e–02	4.4e–02

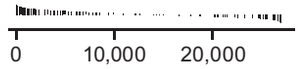

Figure 4.

A, Gene sets enriched in tumor tissue in response to dosing with ivuxolimab from eight paired biopsies of patients dosed with ≥ 1.5 mg/kg indicated that gene sets associated with immune activation and inflammation were among those most enriched (higher positive normalized enrichment score; NES) with the lowest adjusted *P* values. Biopsies were collected at least 2 weeks from last dose. **B,** Gene sets associated with immune activation were among the most enriched in a CT26 syngeneic mouse tumor model. Mice were inoculated subcutaneously with 1 × 105 CT26 cells in 0.1 mL of phosphate-buffered saline (PBS). When tumor volume reached 70 to 100 mm^3, mice were randomized to the anti-OX40 treatment group or the isotype control antibody group.

suggesting diminished clinical activity and T-cell activation at higher doses (e.g., 10 mg/kg) are due to a different mechanism than that of BMS-986178. Moreover, an *in vitro* experiment where ivuxolimab was incubated with human T cells indicated the level of cytokine release peaked at 100 to 1,000 ng/mL of ivuxolimab before declining at higher concentrations (38), similar to that seen clinically with peripheral blood T cells. In our study, tumor RNA-seq analysis revealed enriched gene sets including IFNγ response. It is interesting to speculate that OX40 stimulation with ivuxolimab may lead to activation and infiltration of T cells to the tumor microenvironment, secreting IFNγ upon engaging with their targets.

A positive correlation between OX40-expression change in the tumor and TTP was observed in a limited sample set. Such a correlation with TTP was not observed with baseline levels of OX40, suggesting the antitumor effects of OX40 agonism may both induce and require either increased $OX40^+$ cell infiltration or increased OX40 expression in the tumor microenvironment. These observations imply that increasing OX40 expression by a separate intervention, such as Toll-like receptor activation, may enhance the antitumor activity of OX40 agonism. Also of interest are data showing a potentiation of T-cell response and antitumor activity with the combination of OX40 and vaccine treatment (39, 40).

Interestingly, evaluation of OX40 staining by a medical pathologist, as well as a small follow-up study using *in situ* hybridization on procured RCC samples (data not shown), indicated nonlymphocyte expression of OX40 on dendritic cells (DC) and vascular endothelial

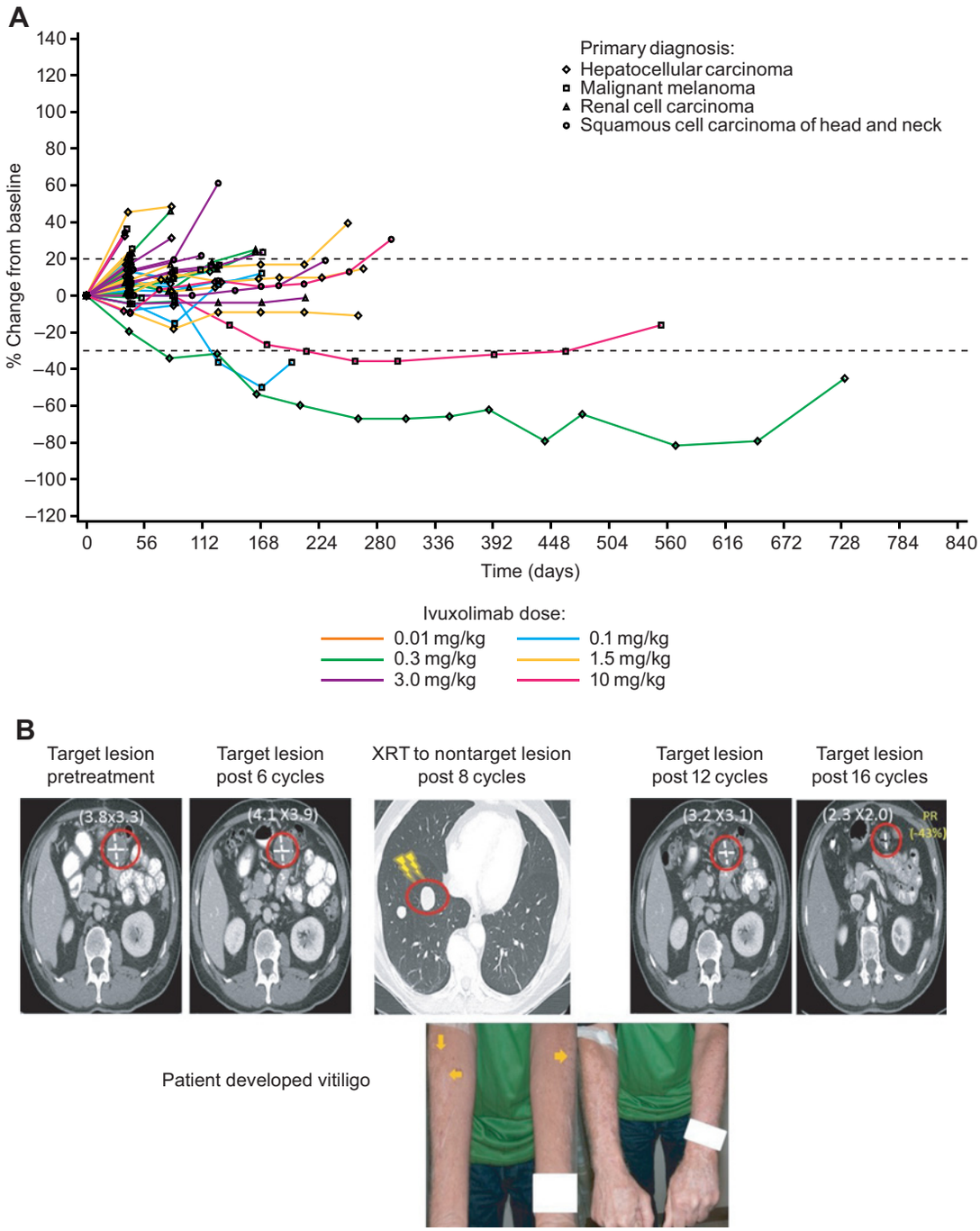

Figure 5.

A, Spider plot of tumor size change from baseline over time by dose and tumor type (RECIST). **B,** Patient receiving ivuxolimab at 10 mg/kg received radiotherapy to a nontarget lesion after 8 cycles and subsequently developed vitiligo. The patient's status was SD after 8 cycles, but by cycle 14 (day 212) of ivuxolimab, the patient achieved a durable PR lasting until cycle 31 (day 462).

cells (VEC). This observation is consistent with results describing increased OX40 expression in tumor-infiltrating $CD11c^+CD11b^+$ DC (TIDC) in MCA205 tumor-bearing mice relative to control DC from tumor-draining lymph nodes (TDLN; ref. 41). Furthermore, when mice were treated with an OX40 ligand–Fc fusion protein, the TIDC upregulated CD80 and CD86 costimulatory receptor ligands and DC levels increased in the TDLN (41). The same study observed OX40 expression on $CD31^+$ VEC and treatment with OX40L–Fc increased VCAM-1 and CXCL9 expression in these cells (41). This provides evidence that engagement of OX40 on DC and VEC by an agonist

molecule may contribute to the increased tumor infiltration of $CD8^+$ T cells, trafficking of costimulation-competent DC to TDLN and vascular normalization observed in this nonclinical study. Assessing if similar mechanistic correlates is observed in patients treated with ivuxolimab will require further correlative clinical biomarker studies. However, this suggests the potential for a nonlymphocyte-mediated component of the mechanism of action of ivuxolimab. Both the correlation of increased OX40 expression with TTP and the contribution of nonlymphocyte OX40 expression must be confirmed and further characterized in follow-up studies of ivuxolimab. Spatial transcriptomic studies will be important to orient OX40 expression with the tumor microenvironment.

RNA-seq analysis of tumor biopsy samples collected at 6 weeks indicated upregulation of gene sets associated with immune activation in the 1.5 mg/kg cohort and above, but not in the 0.1 and 0.3 mg/kg cohorts, where clinical responses were observed. It is important to note that biopsies were not available from patients experiencing a PR at these lower doses. Furthermore, the most enriched gene sets in the ≥1.5 mg/kg dose cohorts were identical to the three most enriched gene sets in a syngeneic mouse tumor model where an ivuxolimab surrogate mAb showed antitumor activity. These data suggest the hypothesis that ivuxolimab induces an inflammatory immune response in the tumor, which, while associated with antitumor activity preclinically, may not be sustained at lower clinical doses that nevertheless mediate significant tumor killing in a subset of patients. Other studies in tumor models have shown evidence of effective OX40-induced T-cell activation associated with antitumor activity such as the A375 melanoma cell model in NOD/SCID mice (42), MCA205-OVA tumor-bearing mice (43), and in mice bearing CT26 tumors (19).

Overall, modest single-agent activity was observed. One immunotherapy-naïve patient with HCC (0.3 mg/kg) and 2 patients with MEL (0.1 and 10 mg/kg) achieved a PR. It is known that HCC is a potential immunoresponsive disease, with a combination of the anti–PD-L1 atezolizumab and bevacizumab becoming a standard treatment modality in selected first-line patients (44). One of the responders with MEL (0.1 mg/kg) had shown progression on prior checkpoint blockade immunotherapy. The other responder with MEL (10 mg/kg) previously had checkpoint blockade halted due to toxicity. This patient was irradiated and subsequently developed vitiligo, which is associated with tumor response in melanoma treated with other immunotherapies (45), then achieved PR based on a nonirradiated target lesion response after 14 cycles of ivuxolimab until cycle 31. Preclinical tumor models suggest that OX40 agonist administration and radiotherapy may have synergy (46–49). A recent study of OX40 stimulation in a murine anti–PD-1-resistant lung tumor model found beneficial outcomes when intratumoral injection of an OX40 agonist antibody followed radiotherapy (46). The combination augmented $CD4^+$ T-cell expansion and induced expression of OX40 on T cells (46). The modest efficacy of OX40 agonist monotherapy may be due to overall low levels of OX40 expression on T cells within the tumor. Hence, strategies to induce OX40 expression in T cells may be important for combination approaches using OX40 agonists.

In conclusion, ivuxolimab was generally well tolerated in patients with select locally advanced or metastatic cancers. PK, immunophenotypic, and RNA-seq data support the on-target biological effects of OX40 targeting and underlie the objective and lasting clinical responses observed in some patients. Supportive pharmacodynamic changes occurred in peripheral T cells and in the tumor, including among prior checkpoint-resistant/refractory patients. The observed efficacy and safety profiles are comparable with those reported for other OX40 agonists such as MEDI0562 (36) and MOXR0916 (50), and similar to results from a phase I study of utomilumab, an agonistic mAb that engages the immune costimulatory molecule 4-1BB (CD137; ref. 51). The AE profile and immune-modulating effects of ivuxolimab provide foundational support to investigate the benefits of modulating costimulatory proteins like OX40, or 4-1BB. In this respect, a phase I study of ivuxolimab with the 4-1BB agonist utomilumab is ongoing in patients with select advanced or metastatic carcinoma. An expansion part of the current study (ivuxolimab 30 mg flat dose) will further assess efficacy, safety, and pharmacodynamics in HCC.

Data and materials availability

Upon request, and subject to certain criteria, conditions, and exceptions (see https://www.pfizer.com/science/clinical-trials/trial-data-and-results for more information), Pfizer will provide access to individual deidentified participant data from Pfizer-sponsored global interventional clinical studies conducted for medicines, vaccines, and medical devices: (i) for indications that have been approved in the US and/or EU or (ii) in programs that have been terminated (i.e., development for all indications has been discontinued). Pfizer will also consider requests for the protocol, data dictionary, and statistical analysis plan. Data may be requested from Pfizer trials 24 months after study completion. The deidentified participant data will be made available to researchers whose proposals meet the research criteria and other conditions, and for which an exception does not apply, via a secure portal. To gain access, data requestors must enter into a data access agreement with Pfizer.

Authors' Disclosures

A. Diab reports grants from Pfizer during the conduct of the study; A. Diab also reports grants from Nektar Therapeutics, BMS, Idera Therapeutics, Merck, and Apexigen, as well as personal fees from Nketar Therapeutics, Apexigen, Pfizer, Iovance, BMS, and Memgen Therapeutics outside the submitted work. O. Hamid reports personal fees from BMS, Novartis, Pfizer, Sanofi Regeneron, Aduro, Akeso, Amgen, Beigene, Bioatla, BMS, Roche/Genentech, GSK, Immunocore, Idera, Incyte, Janssen, Merck, Nextcure, Seattle Genetics, Tempus, and Zelluna, as well as other support from Arcus, Aduro, Akeso, Amgen, Bioatla, BMS, CytomX, Exelixis, Roche/Genentech, GSK, Immunocore, Idera, Incyte, Iovance, Merck, Moderna, Merck-Serono, Nextcure, Novartis, Pfizer, Sanofi Regeneron, Seattle Genetics, Torque, and Zelluna during the conduct of the study. J.A. Thompson reports other support from Pfizer during the conduct of the study. J.A. Thompson also reports other support from Novartis, Five Prime, Merck, Trillium, Incyte, and Xencor; grants from Alpine Biosciences; and personal fees from Regeneron, Aveo, Neoleukin, Calithera, Seattle Genetics, and BJ Biosciences outside the submitted work. F.A.L.M. Eskens reports speaker/teacher honoraria from Pfizer. T. Doi reports grants and personal fees from Taiho, Novartis, MSD, Janssen Pharmaceutical, Sumitomo Dainippon Pharma, Daiichi Sankyo, Bristol Myers Squibb, AbbVie, and Boehringer Ingelheim; grants from Eisai, Pfizer, Chugai Pharmaceutical, Lilly, IQVIA, and Merck-Serono; and personal fees from Rakuten Medical, Amgen, Otsuka Pharmaceutical, Ono Pharmaceutical, Kyowa Kirin, Takeda Pharmaceutical, and Bayer outside the submitted work. S. Hu-Lieskovan reports other support from Pfizer during the conduct of the study, as well as personal fees from Amgen, Genmab, Astellas, Xencor, Regeneron, and BMS outside the submitted work. S.J. Klempner reports personal fees from Eli Lilly, Merck, Bristol Myers Squibb, Astellas, Daiichi Sankyo, Pieris Oncology, and Natera, as well as other support from Turning Point Therapeutics outside the submitted work. C. Fleener reports being a former employee of Pfizer Inc. and holds stock in Pfizer. T. Joh reports other support from Pfizer outside the submitted work. K. Liao reports other support from Pfizer during the conduct of the study, as well as other support from Pfizer outside the submitted work. S. Salek-Ardakani reports stock/stock options at Pfizer. C.T. Taylor reports other support from Pfizer outside the submitted work, and is a colleague of Pfizer. J. Chou reports personal fees and other support from Pfizer during the conduct of the study, as well as personal fees and other support from Pfizer outside the submitted work. A.B. El-Khoueiry reports other support from Pfizer during the conduct of the study. A.B. El-Khoueiry also reports personal fees from Agenus, ABL Bio, Bayer, BMS, Exelixis, Eisai, and AstraZeneca; grants and personal fees from Astex, Pieris, Cytomx, Gilead, EMD Serono, Roche/Genentech, and Merck;

and grants from Fulgent outside the submitted work. No disclosures were reported by the other authors.

Authors' Contributions

A. Diab: Writing–review and editing. **O. Hamid:** Writing–review and editing. **J.A. Thompson:** Writing–review and editing. **W. Ros:** Writing–review and editing. **F.A.L.M. Eskens:** Writing–review and editing. **T. Doi:** Writing–review and editing. **S. Hu-Lieskovan:** Writing–review and editing. **S.J. Klempner:** Writing–review and editing. **B. Ganguly:** Writing–review and editing. **C. Fleener:** Writing–review and editing. **X. Wang:** Writing–review and editing. **T. Joh:** Writing–review and editing. **K. Liao:** Writing–review and editing. **S. Salek-Ardakani:** Writing–review and editing. **C.T. Taylor:** Writing–review and editing. **J. Chou:** Writing–review and editing. **A.B. El-Khoueiry:** Writing–review and editing.

Acknowledgments

This study was sponsored by Pfizer. Medical writing support was provided by David Sunter, PhD, CMPP, of Engage Scientific Solutions and funded by Pfizer. This trial is registered at ClinicalTrials.gov identifier: NCT02315066 (52). The authors acknowledge Susan Pleasic-Williams and Robbin Alpert for flow cytometry analysis, Alison Forgie for additional biomarker data analysis support, Eric Powell for pathology review, Hua Long for preclinical mouse data, Ray Li for additional statistical support, Beihua Fu for his programming support, and Julie Rytlewski from Adaptive for data analysis support. We would also like to acknowledge Cyril Konto, Candy Bermingham, Shobha Potluri, Wenjing Yang, Keith Ching, and Heike Krupka for their support of this body of work.

The costs of publication of this article were defrayed in part by the payment of page charges. This article must therefore be hereby marked *advertisement* in accordance with 18 U.S.C. Section 1734 solely to indicate this fact.

Note

Supplementary data for this article are available at Clinical Cancer Research Online (http://clincancerres.aacrjournals.org/).

Received March 5, 2021; revised June 8, 2021; accepted September 30, 2021; published first October 6, 2021.

References

1. Schachter J, Ribas A, Long GV, Arance A, Grob JJ, Mortier L, et al. Pembrolizumab versus ipilimumab for advanced melanoma: final overall survival analysis of KEYNOTE-006. J Clin Oncol 2016;34:9504.
2. Sharma P, Hu-Lieskovan S, Wargo JA, Ribas A. Primary, adaptive, and acquired resistance to cancer immunotherapy. Cell 2017;168:707–23.
3. Croft M. Control of immunity by the TNFR-related molecule OX40 (CD134). Annu Rev Immunol 2010;28:57–78.
4. al-Shamkhani A, Birkeland ML, Puklavec M, Brown MH, James W, Barclay AN. OX40 is differentially expressed on activated rat and mouse T cells and is the sole receptor for the OX40 ligand. Eur J Immunol 1996;26:1695–9.
5. Paterson DJ, Jefferies WA, Green JR, Brandon MR, Corthesy P, Puklavec M, et al. Antigens of activated rat T lymphocytes including a molecule of 50,000 Mr detected only on CD4 positive T blasts. Mol Immunol 1987;24:1281–90.
6. Mallett S, Fossum S, Barclay AN. Characterization of the MRC OX40 antigen of activated CD4 positive T lymphocytes–a molecule related to nerve growth factor receptor. EMBO J 1990;9:1063–8.
7. Calderhead DM, Buhlmann JE, van den Eertwegh AJ, Claassen E, Noelle RJ, Fell HP. Cloning of mouse OX40: a T cell activation marker that may mediate T-B cell interactions. J Immunol 1993;151:5261–71.
8. Bansal-Pakala P, Halteman BS, Cheng MH, Croft M. Costimulation of CD8 T cell responses by OX40. J Immunol 2004;172:4821–5.
9. Salek-Ardakani S, Moutaftsi M, Crotty S, Sette A, Croft M. OX40 drives protective vaccinia virus-specific CD8 T cells. J Immunol 2008;181:7969–76.
10. Croft M. Co-stimulatory members of the TNFR family: keys to effective T-cell immunity? Nat Rev Immunol 2003;3:609–20.
11. Rogers PR, Song J, Gramaglia I, Killeen N, Croft M. OX40 promotes Bcl-xL and Bcl-2 expression and is essential for long-term survival of CD4 T cells. Immunity 2001;15:445–55.
12. Gramaglia I, Jember A, Pippig SD, Weinberg AD, Killeen N, Croft M. The OX40 costimulatory receptor determines the development of CD4 memory by regulating primary clonal expansion. J Immunol 2000;165:3043–50.
13. Kopf M, Ruedl C, Schmitz N, Gallimore A, Lefrang K, Ecabert B, et al. OX40-deficient mice are defective in Th cell proliferation but are competent in generating B cell and CTL responses after virus infection. Immunity 1999;11:699–708.
14. Song J, Salek-Ardakani S, Rogers PR, Cheng M, Van Parijs L, Croft M. The costimulation-regulated duration of PKB activation controls T cell longevity. Nature Immunol 2004;5:150–8.
15. Song J, So T, Cheng M, Tang X, Croft M. Sustained survivin expression from OX40 costimulatory signals drives T cell clonal expansion. Immunity 2005;22:621–31.
16. Croft M, So T, Duan W, Soroosh P. The significance of OX40 and OX40L to T-cell biology and immune disease. Immunol Rev 2009;229:173–91.
17. Boettler T, Moeckel F, Cheng Y, Heeg M, Salek-Ardakani S, Crotty S, et al. OX40 facilitates control of a persistent virus infection. PLoS Pathog 2012;8:e1002913.
18. Salek-Ardakani S, Flynn R, Arens R, Yagita H, Smith GL, Borst J, et al. The TNFR family members OX40 and CD27 link viral virulence to protective T cell vaccines in mice. J Clin Invest 2011;121:296–307.
19. Piconese S, Valzasina B, Colombo MP. OX40 triggering blocks suppression by regulatory T cells and facilitates tumor rejection. J Exp Med 2008;205:825–39.
20. Vu MD, Xiao X, Gao W, Degauque N, Chen M, Kroemer A, et al. OX40 costimulation turns off Foxp3$^+$ Tregs. Blood 2007;110:2501–10.
21. So T, Croft M. Cutting edge: OX40 inhibits TGF-beta- and antigen-driven conversion of naive CD4 T cells into CD25$^+$Foxp3$^+$ T cells. J Immunol 2007;179:1427–30.
22. Duhen RA, Ballesteros-Merino C, Bell RB, Leidner R, Koguchi Y, Bifulco C, et al. Neoadjuvant OX40 therapy in patients with head and neck cancer induces profound changes in tumor-infiltrating lymphocytes. J Immunol 2018;200:57.40.
23. Duhen R, Ballesteros-Merino C, Frye AK, Tran E, Rajamanickam V, Chang SC, et al. Neoadjuvant anti-OX40 (MEDI6469) therapy in patients with head and neck squamous cell carcinoma activates and expands antigen-specific tumor-infiltrating T cells. Nat Commun 2021;12:1047.
24. Weinberg AD. The role of OX40 (CD134) in T-cell memory generation. Adv Exp Med Biol 2010;684:57–68.
25. Weinberg AD, Rivera MM, Prell R, Morris A, Ramstad T, Vetto JT, et al. Engagement of the OX-40 receptor in vivo enhances antitumor immunity. J Immunol 2000;164:2160–9.
26. Morris A, Vetto JT, Ramstad T, Funatake CJ, Choolun E, Entwisle C, et al. Induction of anti-mammary cancer immunity by engaging the OX-40 receptor in vivo. Breast Cancer Res Treat 2001;67:71–80.
27. Ali SA, Ahmad M, Lynam J, McLean CS, Entwisle C, Loudon P, et al. Anti-tumour therapeutic efficacy of OX40L in murine tumour model. Vaccine 2004;22:3585–94.
28. Sadun RE, Hsu WE, Zhang N, Nien YC, Bergfeld SA, Sabzevari H, et al. Fc-mOX40L fusion protein produces complete remission and enhanced survival in 2 murine tumor models. J Immunol 2008;31:235–45.
29. Redmond WL, Gough MJ, Weinberg AD. Ligation of the OX40 co-stimulatory receptor reverses self-Ag and tumor-induced CD8 T-cell anergy in vivo. Eur J Immunol 2009;39:2184–94.
30. Ji Y, Wang SJ. Modified toxicity probability interval design: a safer and more reliable method than the 3 + 3 design for practical phase I trials. J Clin Oncol 2013;31:1785–91.
31. Love MI, Huber W, Anders S. Moderated estimation of fold change and dispersion for RNA-seq data with DESeq2. Genome Biol 2014;15:550.
32. Sergushichev AA. An algorithm for fast preranked gene set enrichment analysis using cumulative statistic calculation. bioRxiv 2016.
33. Liberzon A, Birger C, Thorvaldsdottir H, Ghandi M, Mesirov JP, Tamayo P. The molecular signatures database (MSigDB) hallmark gene set collection. Cell Syst 2015;1:417–25.
34. Lu P. Monitoring cardiac function in patients receiving doxorubicin. Semin Nucl Med 2005;35:197–201.

35. Curti BD, Kovacsovics-Bankowski M, Morris N, Walker E, Chisholm L, Floyd K, et al. OX40 is a potent immune-stimulating target in late-stage cancer patients. Cancer Res 2013;73:7189.
36. Glisson BS, Leidner RS, Ferris RL, Powderly J, Rizvi NA, Keam B, et al. Safety and clinical activity of MEDI0562, a humanized OX40 agonist monoclonal antibody, in adult patients with advanced solid tumors. Clin Cancer Res 2020;26:5358.
37. Wang R, Gao C, Raymond M, Dito G, Kabbabe D, Shao X, et al. An integrative approach to inform optimal administration of OX40 agonist antibodies in patients with advanced solid tumors. Clin Cancer Res 2019;25:6709–20.
38. Long H, White A, Wei J, Jiang B, Feldman R, Pappas D, et al. Triggering of OX40 on T cells by a novel monoclonal antibody elicits robust antitumor immunity. Cancer Res 2017;77:4598.
39. Malamas AS, Hammond SA, Schlom J, Hodge JW. Combination therapy with an OX40L fusion protein and a vaccine targeting the transcription factor twist inhibits metastasis in a murine model of breast cancer. Oncotarget 2017;8: 90825–41.
40. Yu G, Li Y, Cui Z, Morris NP, Weinberg AD, Fox BA, et al. Combinational immunotherapy with allo-DRibble vaccines and anti-OX40 co-stimulation leads to generation of cross-reactive effector T cells and tumor regression. Sci Rep 2016;6:37558.
41. Pardee AD, McCurry D, Alber S, Hu P, Epstein AL, Storkus WJ. A therapeutic OX40 agonist dynamically alters dendritic, endothelial, and T cell subsets within the established tumor microenvironment. Cancer Res 2010;70:9041–52.
42. Oberst MD, Augé C, Morris C, Kentner S, Mulgrew K, McGlinchey K, et al. Potent immune modulation by MEDI6383, an engineered human OX40 ligand IgG4P Fc fusion protein. Mol Cancer Ther 2018;17:1024–38.
43. Moran AE, Polesso F, Weinberg AD. Immunotherapy expands and maintains the function of high-affinity tumor-infiltrating CD8 T cells in situ. J Immunol 2016;197:2509–21.
44. Finn RS, Qin S, Ikeda M, Galle PR, Ducreux M, Kim TY, et al. Atezolizumab plus bevacizumab in unresectable hepatocellular carcinoma. N Engl J Med 2020;382: 1894–905.
45. Hua C, Boussemart L, Mateus C, Routier E, Boutros C, Cazenave H, et al. Association of vitiligo with tumor response in patients with metastatic melanoma treated with pembrolizumab. JAMA Dermatol 2016;152:45–51.
46. Niknam S, Barsoumian HB, Schoenhals JE, Jackson H, Yanamandra N, Caetano MS, et al. Radiation followed by OX40 stimulation drives local and abscopal antitumor effects in an anti-PD1-resistant lung tumor model. Clin Cancer Res 2018;24:5735–43.
47. Gough MJ, Crittenden MR, Sarff M, Pang P, Seung SK, Vetto JT, et al. Adjuvant therapy with agonistic antibodies to CD134 (OX40) increases local control after surgical or radiation therapy of cancer in mice. J Immunol 2010; 33:798–809.
48. Yokouchi H, Yamazaki K, Chamoto K, Kikuchi E, Shinagawa N, Oizumi S, et al. Anti-OX40 monoclonal antibody therapy in combination with radiotherapy results in therapeutic antitumor immunity to murine lung cancer. Cancer Sci 2008;99:361–7.
49. Young KH, Baird JR, Savage T, Cottam B, Friedman D, Bambina S, et al. Optimizing timing of immunotherapy improves control of tumors by hypofractionated radiation therapy. PLoS One 2016;11:e0157164.
50. Hansen AR, Infante JR, McArthur G, Gordon MS, Lesokhin AM, Stayner A-L, et al. A first-in-human phase I dose escalation study of the OX40 agonist MOXR0916 in patients with refractory solid tumors. Cancer Res 2016;76:CT097.
51. Segal NH, He AR, Doi T, Levy R, Bhatia S, Pishvaian MJ, et al. Phase I study of single-agent utomilumab (PF-05082566), a 4-1BB/CD137 agonist, in patients with advanced cancer. Clin Cancer Res 2018;24:1816–23.
52. ClinicalTrials.gov identifier. NCT02315066. 2014. Available at: https://clinicaltrials.gov/ct2/show/NCT02315066. Accessed July 16, 2020.